Solid State Phenomena
ISSN: 1662-9779, Vol. 359, pp 119-124
doi:10.4028/p-K2pVqU

Submitted: 2023-09-30
Accepted: 2024-04-12
Online: 2024-08-22

Long Term Reliability and Deterioration Mechanisms of High-Temperature Metal Stacks on 4H-SiC

Kevin Brueckner[1,a] and Oleg Rusch[1,b]

[1]Fraunhofer Institute for Integrated Systems and Device Technology IISB, Schottkystr. 10, 91058 Erlangen, Germany

[a]kevin.brueckner@iisb.fraunhofer.de, [b]oleg.rusch@iisb.fraunhofer.de

Keywords: Metallization, High-Temperature, Diffusion Barrier, Ohmic Contact, 4H-SiC.

Abstract. In order to make SiC devices more accessible for high-temperature applications, reliable ohmic contacts and metallization systems which can also withstand extended operation at high temperatures are needed. In this work, metal layer stacks containing Ag, Ti, TiN, Ni and NiAl, where NiAl refers to a mixture of 97,4 wt% Ni and 2,6 wt% Al, were deposited on Si and SiC samples and consecutively thermally aged at 400 °C for 100 h in air. Mesa structures were found to be challenging for keeping oxygen from diffusing through the metal stack to the substrate. On flat surfaces, diffusion barriers were successfully used to protect the ohmic contact on 4H-SiC samples from oxidizing. Diffusion barriers made of TiN were found to show pore formation after the thermal treatment. The reason for the pores is thought to be gas formation, which is believed to be the result of the TiN layers containing too much nitrogen. The exact chemical composition of TiN layers therefore seems to be of vital importance for high-temperature applications.

Introduction

SiC is a promising semiconductor for high-temperature applications. It possesses superior properties, including thermal conductivity, breakdown field strength and Mohs hardness when compared to more commonly used semiconductor materials like Si. Therefore, devices manufactured on SiC have the potential to withstand harsher conditions and be deployed at higher temperatures for extended periods of time [1-3]. Currently, the operating temperatures of SiC devices are not limited by the semiconductor itself, but by the conventional packaging. Materials and components that make up the package typically cannot withstand operating conditions above 200 °C [4]. An essential part of the fully packaged device is the contact metallization, which must not only withstand the elevated temperatures, but should also contain a diffusion barrier to protect the device against reactive species like oxygen [5-6].

In this work, the high-temperature capability of metal layer stacks consisting of Ag, Ti, TiN, Ni and NiAl was investigated. NiAl, Ni and TiN were used to act as diffusion barriers to keep atmospheric oxygen from reaching the nickel silicide at the interface between SiC and the metal stack. Oxygen can react with nickel silicide and degrade the ohmic contact, leading to a considerable performance loss or destruction of the device. Therefore, sufficiently capable diffusion barriers are required to ensure the long-term reliability of the devices when operating at high temperatures [5-6].

Experiment

Processing. The exact layer compositions and thicknesses of the initially deposited layer stacks are shown in Table I. A Clusterline 200 II magnetron sputtering system from Evatec was used to deposit the Ag-Ti-NiAl-Ti-Ag- and the Ag-TiN-Ag-stacks, while the Ag-Ti-Ni-Ti-Ag-stack was deposited using a self-built evaporation system from Fraunhofer IISB. Samples of each stack were thermally aged under atmospheric conditions at 400 °C for 100 h.

Table I. Layer compositions of the high-temperature metal stacks deposited on SiC.

Sample	Layer number				
	1	2	3	4	5
1	Ag 500 nm	Ti 100 nm	NiAl 200 nm	Ti 100 nm	Ag 500 nm
2	Ag 500 nm	Ti 100 nm	Ni 200 nm	Ti 100 nm	Ag 500 nm
3	Ag 1000 nm	TiN 200 nm	Ag 500 nm	-	-

In a second series of tests, the gas composition was varied during the deposition of the TiN layers in order to achieve a favorable stoichiometry. The metal stack of sample 1 was deposited using evaporation, since evaporating metal stacks is the standard procedure for patterning via lift-off. In case of the samples 2 to 4, a TiN target was used. With each sample, the proportion of Ar gas in the reactor chamber was reduced. Samples started at 100 % Ar and went down to 80 % Ar, with the remaining gas being N_2. In contrast to this, for the samples 5 to 8, the TiN layers were created by reactive sputtering using a Ti target. In this case, sample 5 started with a pure N_2 atmosphere. For the samples 6 to 8, the proportion of N_2 in the gas mixture was gradually reduced to 25 %, with the remaining gas being Ar. As with the previous samples, samples of each stack in Table II were thermally aged under atmospheric conditions at 400 °C for 100 h.

Table II. Variations in depositing the TiN-layer of sample 3 in Table I.

Sample	Deposition method	Material	Ar flow rate	N_2 flow rate
1	Reactive evaporation	Ti	20 sccm	20 sccm
2	Sputtering	TiN-Target	100 sccm	0 sccm
3	Sputtering	TiN-Target	90 sccm	10 sccm
4	Sputtering	TiN-Target	80 sccm	20 sccm
5	Reactive sputtering	Ti-Target	0 sccm	33 sccm
6	Reactive sputtering	Ti-Target	10 sccm	30 sccm
7	Reactive sputtering	Ti-Target	20 sccm	20 sccm
8	Reactive sputtering	Ti-Target	30 sccm	10 sccm

After analysis of the samples of Table II, a metal stack containing a TiN layer with the recipe of sample 8 was deposited on SiC MOSFET devices. Deposition was done using a CS 900 S sputtering system from Von Ardenne. Because of restrictions with this sputtering system, the overall gas flow had to be increased to 80 sccm instead of 40 sccm, but the ratio of Ar to N_2 was maintained.

Characterization. Before and after thermal aging, scanning electron microscope (SEM) cross-section images of the samples were analyzed using a Helios Nanolab 600 from Thermo Fisher Scientific. As preparation for imaging, protective Pt layers were deposited on the surface of the samples using the electron beam and subsequently the focused ion beam (FIB). Cross sections of the samples were then prepared via FIB.

Results

In case of the evaporated Ag-Ti-Ni-Ti-Ag-stack, significant degradation could be observed after tempering at 400 °C for 100 h. As shown in Fig. 1 (b), the main mechanism of degradation seems to be the diffusion of oxygen along mesa structures on the patterned front side of the MOSFET, leading to oxidation of the nickel silicide. Interdiffusion between the Ti and Ni layers and pore formation is also present, which is expected to weaken the function as a diffusion barrier. Contrary to this, the sputtered Ag-Ti-NiAl-Ti-Ag-stack, deposited on the backside of the MOSFET, showed much less degradation and intact nickel silicide as seen in Fig. 2 (b). The formation of pores in the NiAl layer is also present, but does not seem to significantly worsen the function as a diffusion barrier in this case. In all deposited layer systems, the top Ag layer underwent island formation and therefore exposed the Ti and TiN layers to atmospheric conditions while at 400 °C. Despite this, the diffusion barriers still functioned as intended, keeping the nickel silicide intact as seen on the left side of Fig. 2 (b).

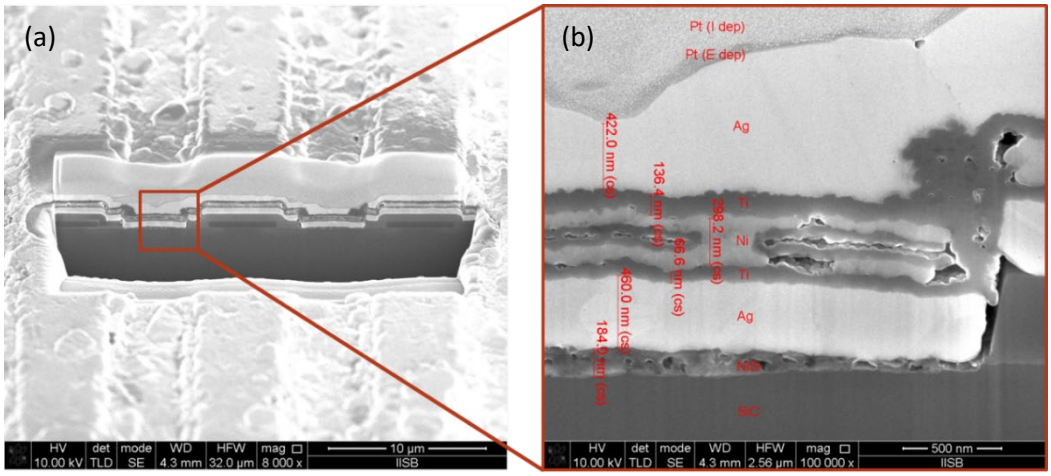

Fig. 1. SEM cross-section image of the evaporated Ag-Ti-Ni-Ti-Ag metal stack on the front side of a SiC MOSFET after thermal treatment at 400 °C for 100 h in air, prepared via FIB and covered by in-situ deposited Pt.

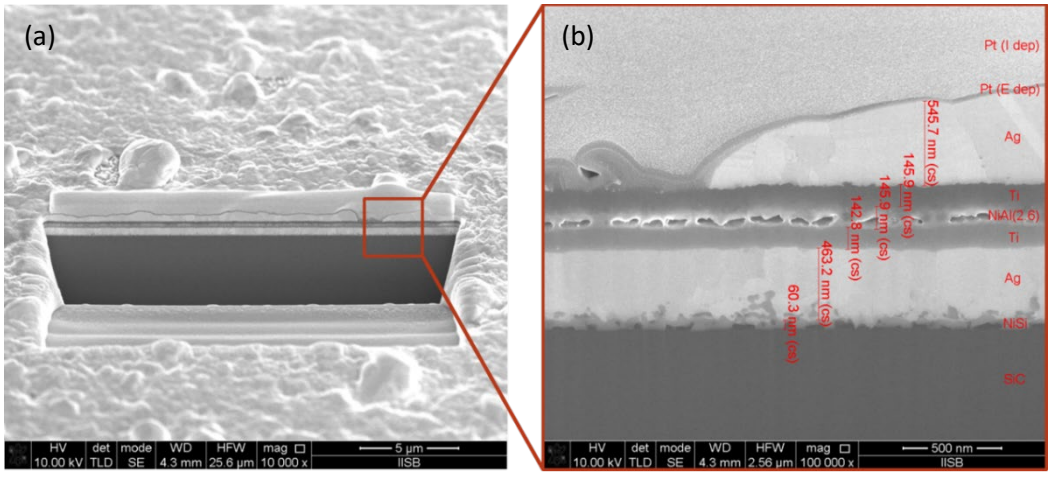

Fig. 2. SEM cross-section image of the sputtered Ag-Ti-NiAl-Ti-Ag metal stack on the back side of a SiC MOSFET after thermal treatment at 400 °C for 100 h in air, prepared via FIB and covered by in-situ deposited Pt.

Out of the samples in Table II, sample 8 turned out to be particularly promising, showing significantly lower TiN layer degradation than the other samples examined. The cross section and the surface of a metal stack using the recipe of sample 8 are shown in Fig. 4 and Fig. 5, respectively. The images were taken after thermal aging at 400 °C for 100 h in air. The cross section of the sample shows pore formation in the Ag layer on top of the nickel silicide as well as in the TiN layer.

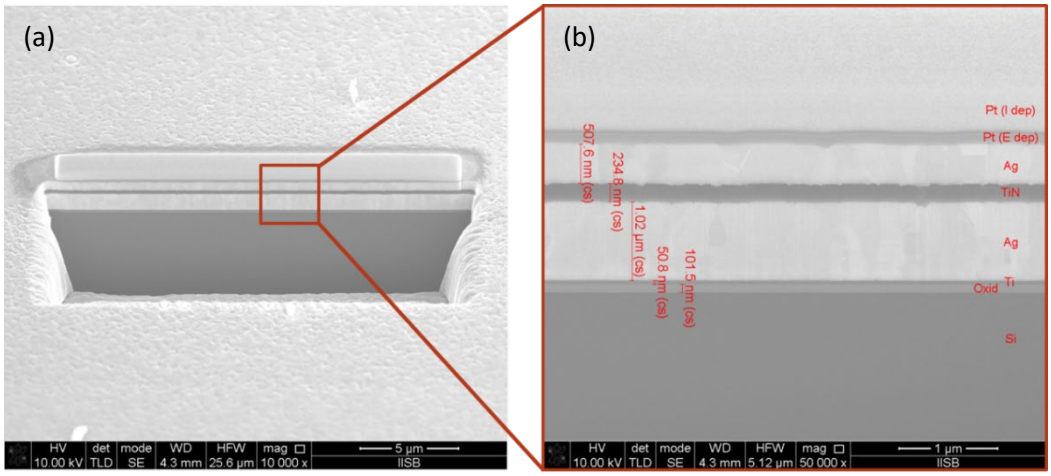

Fig. 3. SEM cross-section image of the sputtered Ag-TiN-Ag metal stack on Si before thermal treatment, prepared via FIB and covered by in-situ deposited Pt.

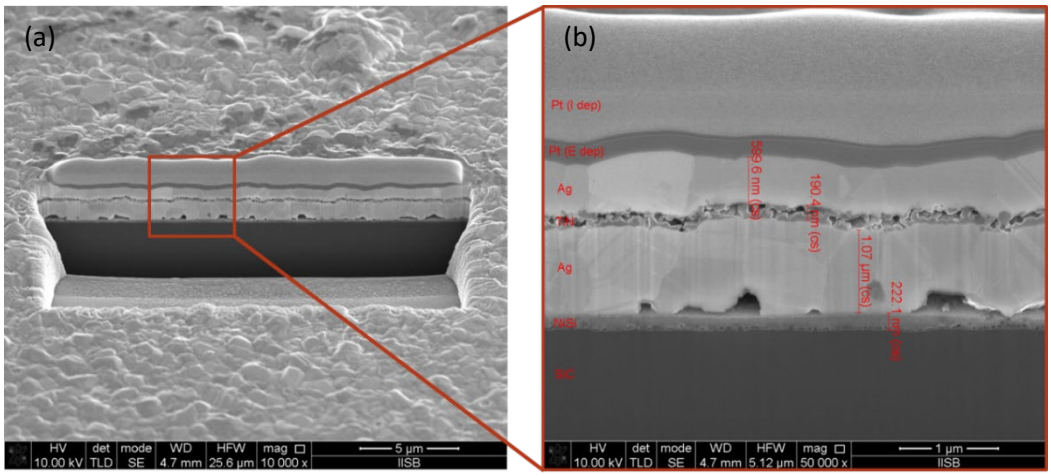

Fig. 4. SEM cross-section image of the sputtered Ag-TiN-Ag metal stack using the recipe of sample 8 on the back side of a SiC chip. Image taken after thermal treatment at 400 °C for 100 h in air, prepared via FIB and covered by in-situ deposited Pt.

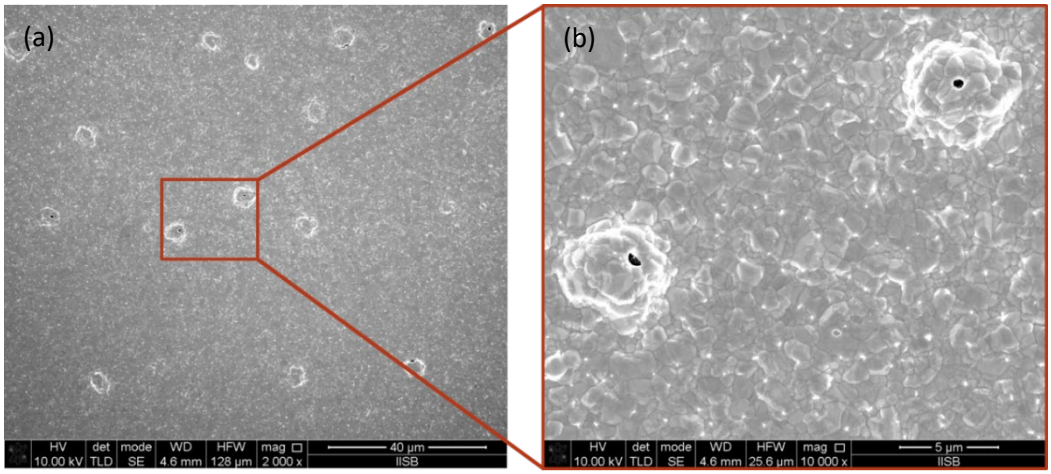

Fig. 5. SEM surface image of the sputtered Ag-TiN-Ag metal stack using the recipe of sample 8 on the back side of a SiC chip. Image taken after thermal treatment at 400 °C for 100 h in air. Visible pore formation, which is thought to be the result of escaping nitrogen gas.

The reason for the porosity of the TiN layer is assumed to be gas formation within the TiN during thermal treatment. The hill-like structures on the surface of the metal stack shown in Fig. 5 also suggest gas formation. Each of the hill-like structures has a small pore from which the gas presumably

escapes. In order to avoid gas formation and thus porosity of the diffusion barrier, the exact chemical composition therefore seems to be essential for high-temperature applications of TiN. It is suspected that the current samples have too much nitrogen content in the TiN, which might cause the gas formation to occur.

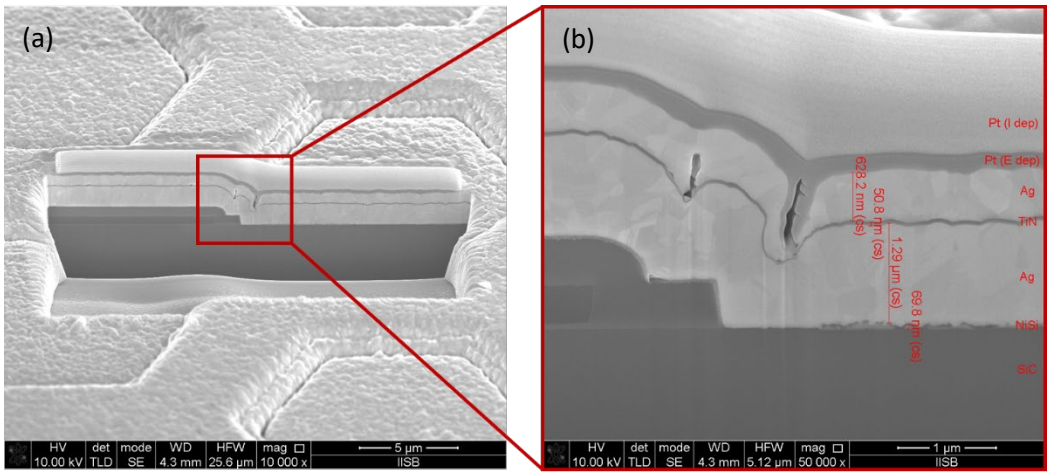

Fig. 6. SEM cross-section image of the sputtered Ag-TiN-Ag metal stack using the recipe of sample 8 on the front side of a SiC MOSFET device. Image taken before thermal treatment, prepared via FIB and covered by in-situ deposited Pt.

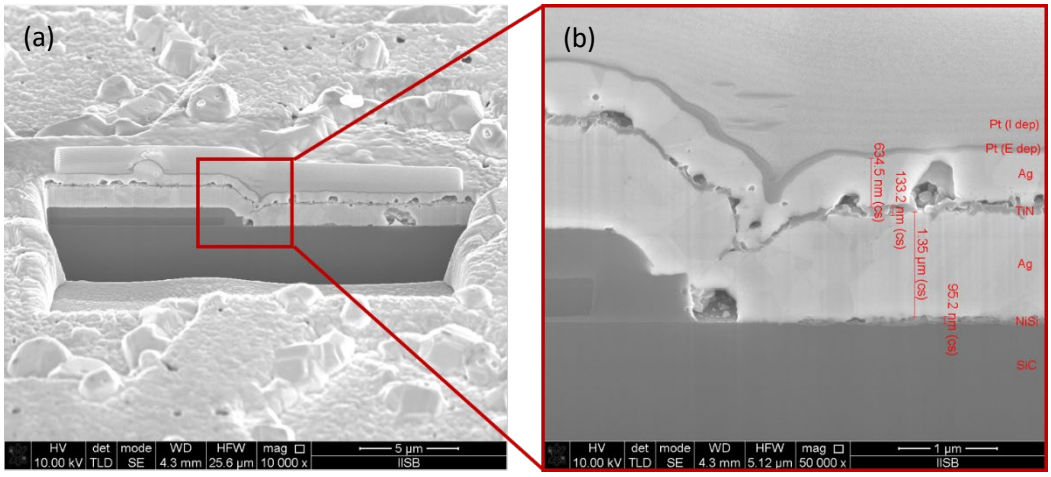

Fig. 7. SEM cross-section image of the sputtered Ag-TiN-Ag metal stack using the recipe of sample 8 on the front side of a SiC MOSFET device. Image taken after thermal treatment at 400 °C for 100 h in air, prepared via FIB and covered by in-situ deposited Pt.

Fig. 6 shows the metal stack on the SiC MOSFET devices after deposition. There is no visible pore formation in the Ag layer deposited directly on the nickel silicide. However, cavities can be seen in the top Ag layer, particularly at the edges of mesa structures. Previous tests have shown that these edges represent weak points for the diffusion of gases such as oxygen and thus for oxidation.

Even though the TiN layer is thinner on the MOSFET devices than on the previously tested Si samples, the TiN still appears to fulfill its function as a diffusion barrier, since no significant degradation of the nickel silicide is visible in Fig. 7 after the thermal treatment. Especially noticeable about this sample is the high number of pores in the Ag layer above the TiN, which, as previously suspected, indicates gas development due to a reaction of the TiN. The porosity within the TiN layer is suspected to occur for the same reason. To a lesser extent, pores are also present in the Ag layer on the nickel silicide, but these are likely not a result of gas formation. Despite the degradation, adhesion was still sufficient, such that no delamination between the metal stack and the substrate occurred.

Summary

In this work, metal layer stacks containing Ag, Ti, TiN, Ni and NiAl were investigated for the use in high-temperature applications. It was found that Ni, NiAl and TiN can all act as sufficient diffusion barriers to protect the nickel silicide at the interface between the metal stack and the substrate from oxidation. Sputtered TiN thin films were previously shown to be stable at high temperatures in metallization systems on SiC [7]. However for the long-term reliability of TiN layers, the exact chemical composition seems to be of vital importance. The current theory is that TiN layers containing too much nitrogen become porous by the formation of nitrogen gas after being exposed to elevated temperatures in air for extended periods of time. TiN layers should therefore only be used as long as a stable composition without gas formation can be achieved. Future work on this topic will focus on further improving the understanding of how TiN layers behave in high-temperature environments. Alternative diffusion barriers, such as TaN and WN will also be investigated.

References

[1] T. Kimoto and J.A. Cooper, Fundamentals of Silicon Carbide Technology, 1st ed. (Wiley, Singapore, 2014), p. 11.

[2] T. Kimoto: Jpn. J. Appl. Phys. Vol. 54 (2015), p. 40103.

[3] B.J. Baliga, Silicon Carbide Power Devices, (World Scientific Publishing, Singapore, 2005), p. 16.

[4] H. Lee, V. Smet and R. Tummala: IEEE J. Emerg. Sel. Topics Power Electron. Vol. 8 (2020), p. 239.

[5] A.V. Kuchuk, M. Guziewicz, R. Ratajczak, M. Wzorek, V.P. Kladko and A. Piotrowska: Microelectronic Engineering Vol. 85 (2008), p. 2142.

[6] A.V. Adedeji, A.C. Ahyi, J.R. Williams, S.E. Mohney and J.D. Scofield: Solid-State Electronics Vol. 54 (2010), p. 736.

[7] Dela Cruz, Zhongtao Wang, Ping Cheng, Carlo Carraro and Roya Maboudiana: Thin Solid Films Vol. 670 (2019), p. 54.